Am J Transl Res 2020;12(5):1928-1941
www.ajtr.org /ISSN:1943-8141/AJTR0095786

Original Article

The polymorphism of rs11614913 T/T in pri-*miR-196a-2* alters the miRNA expression and associates with recurrent spontaneous abortion in a Han-Chinese population

Xueqin Wang[1,2,3], Lu Zhang[1,3], Chunyi Guan[1,3], Yichao Dong[1,3], Haining Liu[2], Xu Ma[1,3], Hongfei Xia[1,3]

[1]Reproductive and Genetic Center of National Research Institute for Family Planning, Beijing, China; [2]Department of Reproductive Medicine, Qingdao Municipal Hospital, Qingdao University, Qingdao, Shandong, China; [3]Graduate School, Peking Union Medical College, Beijing, China

Received April 21, 2019; Accepted January 17, 2020; Epub May 15, 2020; Published May 30, 2020

Abstract: Rs11614913 in pri-*miR-196a-2* is involved in the occurrence of many diseases, especially in cancers. However, it remains unknown whether *miR-196a-2* is associated with human recurrent spontaneous abortion (RSA) in Chinese Han population. Our study found that rs11614913 T/T in pri-*miR-196a-2* was associated with the increase risk of human unexplained RSA (URSA) in recessive mode in Chinese Han population. The T allele of rs11614913 increased the production of mature *miR-196a-3p*. Rs11614913 T/T inhibited HTR-8/SVneo cells proliferation and migration and promoted cells apoptosis. Further investigation discovered that dihydrofolate reductase (*DHFR*) was the target of *miR-196a-3p* and inversely regulated by *miR-196a-3p*. Dual-luciferase assay indicated that T allele in *miR-196a-2* rs11614913 could more effectively suppress *DHFR* expression than C allele. In addition, C to T substitution in *miR-196a-2* rs11614913 attenuated the sensibility of cells to mifepristone. Collectively, our data suggest that *miR-196a-2* rs11614913 T/T in pri-*miR-196a-2* may be conductive to the genetic predisposition to RSA by disrupting the production of mature *miR-196a-3p* and reinforcing the expression of *DHFR*.

Keywords: *miR-196a-2*, rs11614913, recurrent spontaneous abortion, trophoblast

Introduction

Recurrent spontaneous abortion (RSA), defined as loss of two or more consecutive pregnancies before 20th week and this definition makes the percentage of RSA to 5% [1]. The causes of RSA have been generally recognized to include anatomical issues, genetics and hormonal abnormalities, exposure to environmental factors, infection, smoking and alcohol consumption, psychological trauma and stressful life events and immune regulatory protein defects [2]. However, at least 50% of RSA patients have no deviation [3, 4]. The regions of genomes polymorphisms associated with RSA are mainly focused on coding RNAs [5]. Limited knowledge is available about the association between polymorphisms in non-coding RNAs (ncRNAs) and RSA.

The placenta, a maternal-fetal barrier, provides the developing fetus with all of the nutrients necessary for its development [6]. Increasing researches focus on the placenta and abnormal pregnancy. During pregnancy, the proliferation and apoptosis of placenta trophoblasts are closely regulated in a dynamic balance, if the balance is disturbed, apoptosis will predominate in the trophoblast cell growth process, resulting in abnormal placental development, aberrant fetal growth and adverse pregnancy outcomes [7].

MicroRNAs (miRNAs) represent a recently discovered class of small regulatory RNAs that elicit critical changes in gene expression programs that underlie diverse aspects of biology, such as embryogenesis and regulation of cellular differentiation, metabolism, proliferation and apoptosis [7]. Recent studies have clearly demonstrated that single nucleotide polymorphisms (SNPs) within the miRNA sequence may affect miRNA processing and modulate miRNA expression [8, 9], eventually lead to the occur-

rence of diseases. An increasing number of studies have demonstrated that miRNAs are expressed abundantly in the human placenta, and dysregulation of miRNAs has been associated with RSA pathogenesis [4, 10]. The well-known miRNA polymorphism in pre-miRNA sequences, miR-196a-2 rs11614913 has been extensively studied and were found to be associated with the risk and/or prognosis of various diseases [11, 12]. Jeon reported that *miR-196a-2* CC is significantly associated with idiopathic recurrent spontaneous abortion (RSA) in Korean women [13]. However, no data has been reported regarding the role of the *miR-196a-2* rs11614913 polymorphisms in the pathogenesis and role of RSA in Chinese Han population.

In this study, we explored the relationship between *miR-196a-2* rs11614913 and URPL. We found that *miR-196a-2* rs11614913 T/T was verified to be associated with an increased risk of URPL and could significantly increase the production of mature *miR-196a-3p* and promote trophoblast cells apoptosis by targeting *DHFR*. C to T substitution in *miR-196a-2* rs11614913 attenuated the sensibility of cells to mifepristone, but not progesterone.

Materials and methods

Subjects

Blood samples of 300 RPL and 313 controls were collected from Peking Union Medical College Hospital. All patients with RPL had no known causes, and had experienced at least two spontaneous miscarriages and no successful history of pregnancy. The age-matched control groups had a regular menstrual cycles, no history of pregnancy loss, and a history of at least one naturally conceived pregnancy or karyotype 46, XX. All possible cause of abortion, including congenital, infectious, chromosomal, immunological, hormonal and anatomical pathologies were examined to exclude both in RPL and control groups. The study protocol was approved by the Ethics Committee of the National Research Institute for Family Planning. Informed consent were obtained from all participants.

Genotyping of miR-196a-2 C>T

Genomic DNA from URPL patients and controls peripheral blood and cell lines were extracted by EasyPure Genomic DNA Kit (Transgene Biotech, Beijing, China). *MiR-196a-2* C>T genotypes were analyzed using polymerase chain reaction (PCR) and direct sequencing. Primer sequences for PCR amplification of the polymorphism to generate a 447-bp product were as follows: forward 5'-CAGACCCCTTACCCACCCAGC-3' and reverse 5'-GACTCCTCTC CCTTAATCACA-3'. The PCR products were sequenced in forward direction with the ABI 3730xl sequencing platform. Allele and genotype frequencies were calculated using SHESIS online software package (www.shesis.org) by chi-square test.

Cells culture and transfection

HEK-293, HEC-1B, HEK-293T, JEG-3 and Hela cells were obtained from Chinese Academy of Medical Sciences. Placental trophoblast cell lines HTR-8/SVneo were presented from Graham [11]. HEK-293, HEK-293T and Hela cells were grown in DMEM high glucose medium (Hyclone, Australia), and Hec-1B and HTR-8/SVneo cells in RPMI1640 (Hyclone, Australia) medium, supplemented with 10% FBS (HyClone, Australia) and 1% penicillin/streptomycin at 37°C with 5% CO_2. HTR-8/SVneo cells were plated before transfection, and transfection was performed using lipofectamine 2000 (Invitrogen, Carlsbad, CA, USA) according to the manufacture's instruction.

Quantitative reverse-transcriptase polymerase chain reaction (qRT-PCR)

Total RNAs were isolated using Trizol reagent (Invitrogen, Carlsbad, CA, USA). The expression of *miR-196a-3p*, *miR-196a-5p* and *DHFR* were performed using the iScript cDNA Synthesis Kit (Bio-Rad, Hercules, CA, USA) and FastStart Univel SYBR Green Master (Roche, Mannheim, Germany). QRT-PCR primers for miR-196a-3p AND miR-196a-5p were purchased from Guangzhou RiboBio Co. qRT-PCR primers for *DHFR* were as follows: 5'-GCCACCGCTCAGGAATGAAT-3' and 5'-GAGCTCCTTGTGGAGGTTCC-3'. β-ACTIN was the endogenous reference for *DHFR* quantification experiments. QPCR was amplified and quantified on the 7500 Sequence Detection System (Applied Biosystems). The relative expression of *miR-196a-5p*, *miR-196a-3p* and *DHFR* were calculated using the $2^{-\Delta\Delta ct}$ method. All reactions were run in triplicate and relative gene expression. One-way analysis of

variance (ANOVA) was used to analyze the differences among groups.

EdU incorporation assay

HTR-8/SVneo cells were transfected with PCR-3.1, *miR-196a-2*-T/T, *miR-196a-2*-C/C or *miR-196a-2*-T/C to investigate the effects of different genotypes on the cell proliferation. Subsequently, cells were incubated with 50 μM 5-ethynyl-2-deoxyuridine (EdU) (Ribobio, Guangzhou, China) for an additional 2 h. The following steps were conducted according to manufacturer's instructions as previously described [27]. Cells were visualized and imaged under a laser-scanning confocal microscope (CarlZeiss LSM 710 META, Germany) in at least five random fields per well at ×400 magnification. Cells proliferation rate was described as a ratio of the cell number with proliferative cells vs total cells. One-way analysis of variance (ANOVA) was used to analyze the differences among groups.

Cell viability assay

Effects of different genotypes on the cell proliferation was further confirmed by MTT assays. HTR-8/SVneo cells were seeded in triplicate in 96-well plates overnight. 48 hours after transfection, 20 μL MTT (0.5 mg/ ml) (Sigma, St. Louis, MO, USA) solution was added to each well and incubation for 4h at 37°C. Dimethyl sulfoxide (DMSO) was used to dissolve the Formosan. The absorbance (OD) at 570 nm was determined by a Model 3550 microplate reader (Bio-Rad). Cell viability was described as a ratio of OD with different genotypes vs empty PCR3.1 control. One-way analysis of variance (ANOVA) was used to analyze the differences among groups.

Apoptosis assay

HTR-8/SVneo cells were transfected with PCR3.1, *miR-196a-2*-T/T, *miR-196a-2*-C/C and *miR-196a-2*-T/C in 12-well plates. After 48 hours, cells were harvested and diluted in 100 μl 1× annexin V-binding buffer. Then cells were stained with 5 μl Annexin V and 1 μl PI for 15 min (Invitrogen, Carlsbad, CA USA). 400 μl 1× annexin V-binding buffer was added into each sample before detection. Apoptosis were analyzed by FACS Calibur system (BD Biosciences, USA) and 10,000 events were collected for each sample. The experiment was repeated for three times. One-way analysis of variance (ANOVA) was used to analyze the differences among groups.

Transwell migration and invasion assays

HTR-8/SVneo cells were seeded in 24-well plates overnight and transfected with PCR3.1, *miR-196a-2*-T/T, *miR-196a-2*-C/C and *miR-196a-2*-T/C. 48 hours after transfection, cells were harvested and counted for further assays. Cell migration (without Matrigel) and invasion assays (with Matrigel, BD, Biosciences) were performed using transwell chambers (Coring, New York, USA) as described previously [27]. Cells on the top side of the membrane were washed off, and cells on the bottom of membrane were fixed with 4% formaldehyde and stained with crystal violet (Sigma-Aldrich, USA), and counted in at least five different fields at the ×400 magnification. One-way analysis of variance (ANOVA) was used to analyze the differences among groups.

Plasmid construction and luciferase reporter assay

To generate *miR-196a-2* over-expression constructs, a 1110-bp fragment containing 500 bp up and downstream of the pre-miR-196a-2 was amplified from Hela cells complementary DNA (cDNA) by PCR using 5'-CCCAAGCTTTGATTGGAAGTGGCTCCAGAGCACA-3' (forward) and 5'-GCTCTAGACAACTCTTGGAACCTCCAGGTAC-3' (reverse) and cloned into PCR3.1 vector with *KpnI* and *XbaI* restriction enzyme sites. Fast mutagenesis system (Transgene Biotech, Beijing) was used to construct different genotype vectors. The 3'UTR containing *miR-196a-3p* target sites was amplified from human genomic cDNA with *NheI* and *SalI* flanked primers (5'-GGGGTACCCTCTTCTTGGAGATTTTCACTTG-3' and 5'-ACGCGTCGACAGGCAGGAGAATCGCTTGAATCTG-3') and then cloned into pmiR-GLO dual-luciferase miRNA target expression vector (Promega, Madison, WI, USA) (called *DHFR*-pmiRGLO). All constructions were confirmed by direct sequencing. For the luciferase assay, HEK-293T cells were transfected with *miR-196a-3p* mimic or inhibitor and *DHFR*-pmiRGLO or *DHFR*-pmiRGLO-mut. Luciferase activity was analyzed using the Dual-Luciferase Assay (Promega, Madison, WI, USA). The results were described as a relative luciferase activity (Firefly

LUC/Ranilla LUC). At least three replicates with three independent experiments were performed. One-way analysis of variance (ANOVA) was used to analyze the differences among groups.

Protein extraction and western blotting

For western blotting, HTR-8/SVneo cells were transfected with *miR-196a-3p* mimic or inhibitor. 48 hours after transfection, cells were lysed with RIPA buffer containing phenylmethanesulfonyl fluoride (PMSF). Protein lysates in each sample were resolved by SDS-PAGE to the polyvinylidene fluoride (PVDF) membrane (Amersham Pharmacia Biotech, St. Albans, Herts, UK). The membranes were blocked with 5% non-fat milk and probed overnight at 4°C with anti-*DHFR* (Bioworld Technology, USA) and anti-*β-ACTIN* (Santa Cruz Biotechnology Inc., Santa Cruz, CA USA) respectively. Immunoreactive proteins were visualized with HRP-labeled secondary antibodies and detected with the ECL system (Pierce, Appleton, WI USA). Quantification was analyzed by Quantity-One software (Bio-Rad, Hercules, CA, USA) and one-way analysis of variance (ANOVA) was used to analyse the differences among groups. The experiment was repeated for three times.

Data analysis

Allele and genotype frequencies were calculated using SHESIS online software package (www.shesis.org) by chi-square test. Other data were analyzed by the SPSS 19.0 (SPSS Inc., Chicago, IL, USA). Unpaired Student's t-tests were used to compare differences between two groups. Multiple group's comparisons were analyzed by One-way analysis of variance (ANOVA). $P<0.05$ was considered significant.

Results

Association of miR-196a-2 rs11614913 and URPL in the Chinese Han Population

The sequencing of rs11614913 were shown in **Figure 1A**. The distributions of rs11614913 was in Hardy-Weinberg equilibrium in RSA group ($P=0.51$; $\chi^2=0.43$, **Table 1**) and controls ($P=0.87$; $\chi^2=0.03$, **Table 1**). Subjects with rs11614913 TT genotype had a higher RSA risk compared with subjects carrying C/C genotype (OR=1.54, 95% CI, 1.00-1.75, $P=0.026$). Rs11614913 showed a marginal association (OR=1.35, 95% CI, 0.91-2.17, $P=0.057$) in dominant model (T/C+T/T vs. C/C), and significant association in a recessive model (C/C+T/C vs. T/T, OR=1.54, 95% CI, 1.09-2.17, $P=0.01$) and additive model (C/C vs T/T, OR=1.82, 95% CI, 1.56-2.86, $P=0.009$) (**Table 1**).

MiR-196a-2 secondary structure prediction

The secondary structure of 1,104 bp pri-*miR-196a-2* sequence including pre-miRNAs and 500 bp upstream and downstream, was predicted using RNAfold web server (rna.tbi.univie.ac.at/cgi-bin/RNAfold.cgi). The rare allele T doesn't cause a change in loop size but a lowering of the predicted thermodynamic ensemble free energy (ΔG) from -452.90 kcal/mol to -447.30 kcal/mol (**Figure 1B**). Bigger absolute value of ΔG means more instable RNA secondary structural in spite of no obvious differences between the two figures in **Figure 1B**. Therefore, we speculate that rs11614913 in pre-*miR-196a-2* may impact the function of mature *miR-196a-5p* and/or *miR-196a-3p*.

MiR-196a-5p and miR-196a-3p expression from different genotypes in transfected cells

Transfected cells with different genotypes significantly increase the level *miR-196a-5p* compared with PCR3.1 vectors (**Figure 1C**, $P<0.01$), but no differences were found among different genotypes. Rs11614913 C>T located in +78 relative to the first nucleotide of pre-*miR-196a-2* and +17 relative to the first nucleotide of *miR-196-3p* (**Figure 1E**), which indicating that the polymorphism could influence the formation of *miR-196-3p*, then *miR-196-3p* expression level was detected (**Figure 1D**). Compared with PCR3.1 vectors, transfected cells with different genotypes significantly increase the level *miR-196a-3p* ($P<0.01$). Compared with the C allele, T allele significantly increased the expression level of mature *miR-196a-3p* ($P<0.01$). Mature *miR-196a-3p* level was significantly lower in T/C heterozygosity than that in T allele ($P<0.05$) and higher than that in C allele ($P<0.01$). These results uncover that C to T substitution in *miR-196a-2* rs11614913 is conducive to the production of mature *miR-196a-3p* but not *miR-196a-5p*.

MiR-196a-3p expression and genotypes in different cell lines

The genotypes of *miR-196a-2* rs11614913 in HEK-293, HELA, HEK-293T, HEC-1B, JEG-3 and

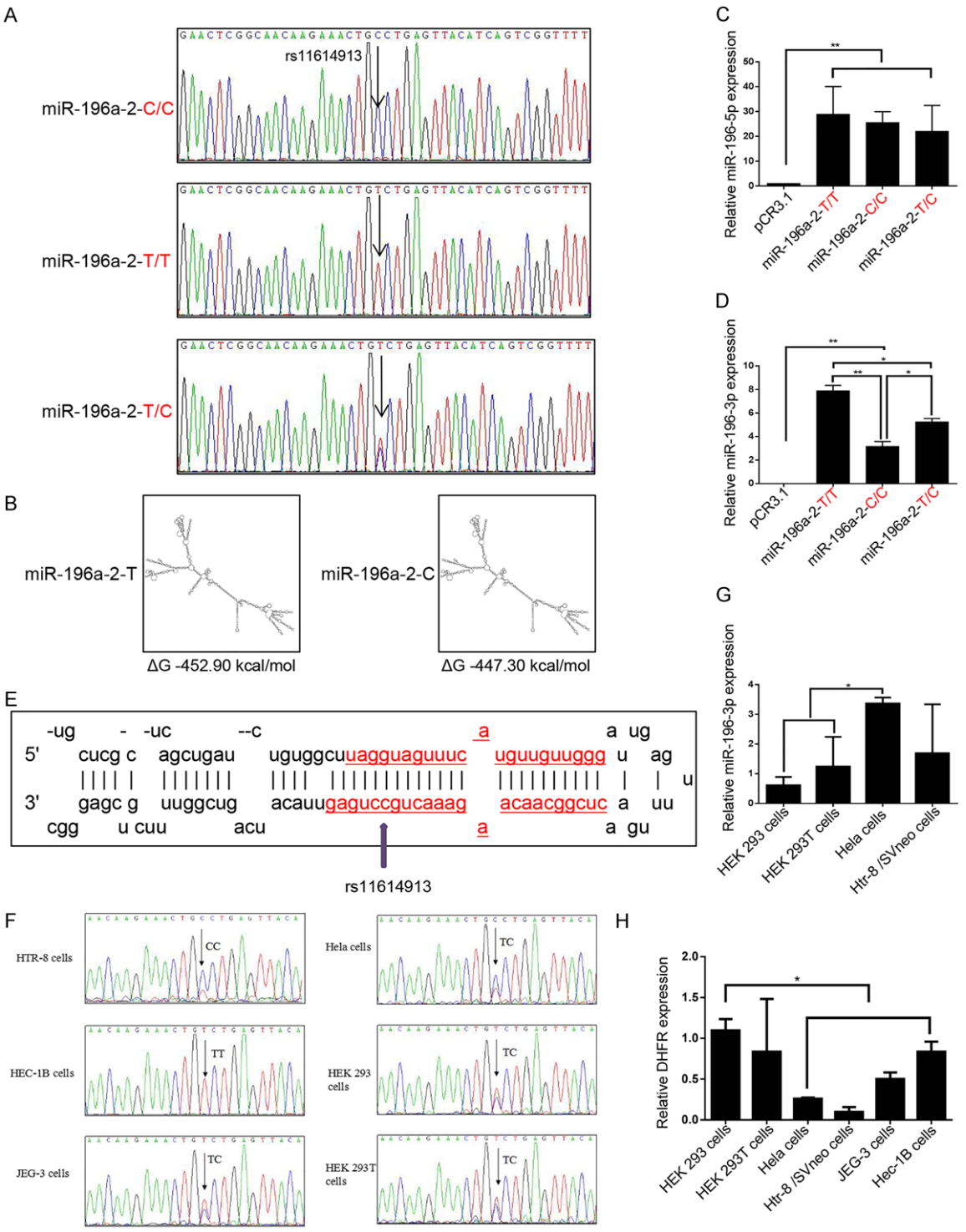

Figure 1. Sequencing, secondary structure prediction and expression detection of pri-196a-2. (A) An example of chromatographs showing the different genotypes on rs11614913 in pri-*miR-196a-2*. Black arrows indicate the SNP site. (B) Predicted secondary structure of pri-*miR-196a-2* indicated that the allele T doesn't cause a change in loop size but a lowering of the predicted thermodynamic ensemble free energy. (C) *miR-196a-5p* and *miR-196a-3p* (D) level was detected in cells transfected with the empty PCR3.1 vector and different genotypes vectors by qRT-PCR. C to T substitution in miR-196a-2 rs11614913 is conducive to the production of mature miR-196a-3p but not miR-196a-5p. (E) Nucleotide sequence of *miR-196a-2*. Rs11614913 is marked with arrow head. The two mature sequences (*miR-196a-5p* and *miR-196a-3p*) are underlined and marked in red. (F) The alleles of *miR-196a-2* rs11614913 in different cell lines were detected by sequencing. The relative expression of *miR-196a-3p* (G) and DHFR (H) in different cell lines. **P*<0.05, ***P*<0.01.

Table 1. SNP genotype distribution and allele frequencies

	RSA (n=300)	Control (n=313)	OR 95% CI	*P*
Alleles/Genotypes				
C	248 (0.413)	307 (0.490)	0.73 (0.58-0.92)	0.0067
T	352 (0.587)	319 (0.510)	1.37 (1.09-1.71)	
C/C	54 (0.180)	76 (0.243)	0.79 (0.52-1.19)	0.026
T/C	140 (0.467)	155 (0.495)	0.89 (0.65-1.22)	
T/T	106 (0.353)	82 (0.262)	1.54 (1.09-2.17)	
Recessive model				
C/C+T/C	194 (0.647)	231 (0.738)	0.65 (0.46-0.92)	0.01
T/T	106 (0.353)	82 (0.262)	1.54 (1.09-2.17)	
Dominant model				
C/C	54 (0.180)	76 (0.243)	0.68 (0.46-1.01)	0.057
T/C+T/T	246 (0.820)	237 (0.757)	1.35 (0.91-2.01)	
Addictive model				
C/C	54 (0.180)	76 (0.243)	0.55 (0.35-0.86)	0.009
T/T	106 (0.353)	82 (0.262)	1.82 (1.56-2.86)	
HWE (*P*)	0.51	0.87		

OR, odd ratio; 95% CI, 95% confidence interval; HWE, Hardy-Weinberg equilibrium.

HTR-8/SVneo cells was detected by PCR and direct sequencing. The genotype was C/C in HTR-8/SVneo cells, and T/C in HEC-1B, HELA, JEG-3, HEK-293 and HEK-293T cells (**Figure 1F**). Mature *miR-196a-3p* expression in HEK-293, HELA, HEK-293T, HEC-1B, JEG-3 and HTR-8/SVneo cells was detected by TaqMan miRNA qRT Real-Time PCR. The expression level of *miR-196a-3p* in Hela cells was significantly higher than that in HEK-293 and HEK-293T cells, and slightly higher than in HTR-8/SVneo cells (**Figure 1G**). Cycle threshold (CT) values were undetermined in JEG-3 cells and HEC-1B cells.

MiR-196a-2 rs11614913 T/T inhibits cell proliferation

HTR-8/SVneo cells were transfected with PCR3.1, *miR-196a-2*-T/T, *miR-196a-2*-C/C or *miR-196a-2*-T/C. After 48 h, MTT and Edu assays were used to evaluate cell proliferation (**Figure 2A** and **2B**). Compared with the empty PCR3.1 vector, the T/T homozygote significantly weakened the proliferation rate ($P<0.01$) in Edu assay. The proliferation rates in C/C homozygote were significantly higher than that in T/T homozygote and T/C heterozygosity ($P<0.05$). To further confirm the role of *miR-196a-3p* in cell viability, the proliferation capacity of HTR-8/SVneo cells was determined by the MTT assay (**Figure 2B**). The results were similar with Edu assay. These results show that the T allele inhibits cell proliferation relative to C allele.

MiR-196a-2 rs11614913 T/T increases cell apoptosis

Flow cytometry was used to analyze the apoptosis in HTR-8/SVneo cells transfected with PCR3.1, *miR-196a-2*-T/T, *miR-196a-2*-C/C or *miR-196a-2*-T/C. The cell apoptotic level in early stage in PCR3.1 and *miR-196a-2*-T/T was obviously higher than that in *miR-196a-2*-C/C (**Figure 2C** and **2C1**), while no significant differences existed in late stage among three genotypes (**Figure 2C** and **2C2**). Total apoptotic cells in *miR-196a-2*-T/T was obviously higher than that in *miR-196a-2*-C/C (**Figure 2C** and **2C3**). These results further prove that the *miR-196a-2*-T/T in pre-*miR-196a-2* is not favorable for trophoblast cell survival.

MiR-196a-2 rs11614913 T/T represses cell migration

In order to investigate the roles of *miR-196a-2* rs11614913 in cell migration and metastasis-related behaviors, the transmembrane migration and invasive assay was performed (**Figure 3A** and **3B**). The results indicated that *miR-196a-2*-T/T in *pre-miR-196a-2* represses cell migration compared with *miR-196a-2*-C/C and *miR-196a-2*-T/C ($P<0.05$, **Figure 3A** and **3A1**). Similarly, *miR-196a-2*-T/T represses cell invasion compared with the empty PCR3.1 ($P<0.05$). However, *miR-196a*-2-C/C represses cell invasion compared with *miR-196a*-2-T/T and *miR-196a*-2-T/C ($P<0.05$) (**Figure 3B** and **3B1**).

MiR-196a-3p directly targets the 3'-UTR of DHFR

The targets of *miR-196a-2* were predicted using target prediction programs online by TargetScan (www.targetscan.org) and miRDB (http://mirdb.org/miRDM/index.html). We chose dihydrofolate reductase (*DHFR*) and thymi-

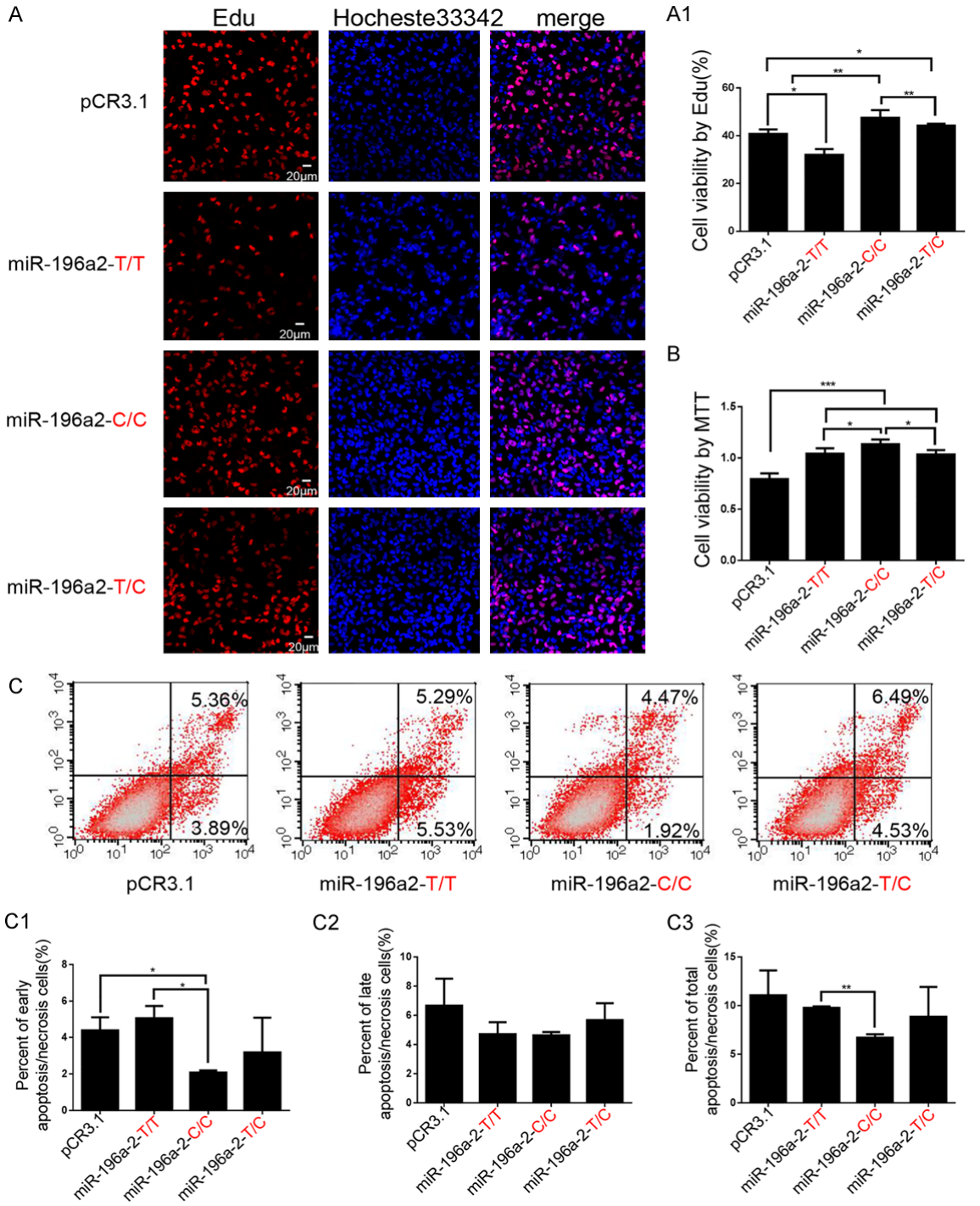

Figure 2. *MiR-196a-2* rs11614913 T/T inhibits cell proliferation and increases cell apoptosis. Cell proliferation was determined by EdU assay (A and A1) and MTT assay (B). T allele inhibits cell proliferation relative to C allele. Red represents the proliferative cells. Blue indicates cell nuclei. The photographs were shown at ×400 original magnification. (C) Cell apoptosis was detected by flow cytometry analysis. The percentages of early and late apoptotic cells (representatives of three separate experiments) are shown in the lower right and upper right panels respectively. Histogram of percentage of (C1) early apoptotic, (C2) late apoptotic and (C3) total apoptotic cells were shown. The *miR-196a-2*-T/T in pre-*miR-196a-2* is not favorable for trophoblast cell survival. **P*<0.05, ***P*<0.01.

dylate synthase (*TYMS*) from a large number of putative mRNA targets for the following reasons: there is a conservative 7nt *miR-196a-3p* responsive element in 3'UTR of *DHFR* and

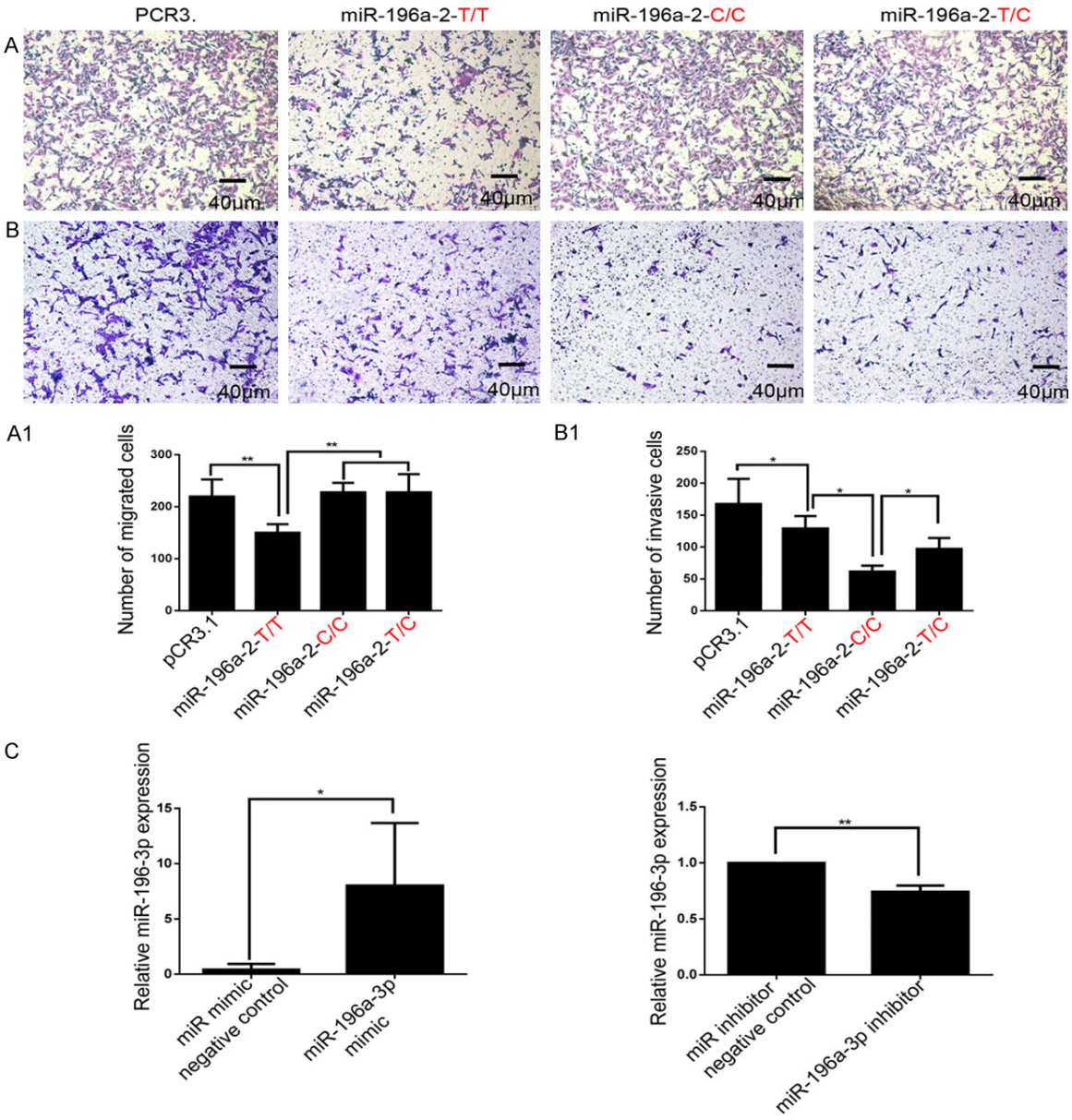

Figure 3. *MiR-196a-2* rs11614913 T/T represses cell migration. Photomicrographs of migration (A) and invasion (B) cells 24 h after inoculation. Histogram of number of migration (A1) and invasion (B1) cells through filters. *MiR-196a-2-T/T* in *pre-miR-196a-2* represses cell migration compared with *miR-196a-2*-C/C and *miR-196a-2*-T/C. However, *miR-196a*-2-C/C represses cell invasion compared with *miR-196a*-2-T/T and *miR-196a*-2-T/C. Data are expressed as the mean numbers of independent triplicate experiments. (C) *MiR-196a-3p* expression detection in HTR-8/SV-neo cells after transfected with *miR-196a-3p* mimic or *miR-196a-3p* inhibitor. **P*<0.05, ***P*<0.01.

TYMS (**Figure 4A**). *DHFR* converts dihydrofolate into tetrahydrofolate, a methyl group shuttle required for the *de novo* synthesis of purines, thymidylic acid, and certain amino acids [14]. *TYMS* catalyzes the methylation of deoxyuridylate to deoxythymidylate, using 10-methylenetetrahydrofolate (methylene-THF) as a cofactor [15]. Dysfunction of *DHFR* and *TYMS* are related to folic acid metabolism abnormality, which is involved in the occurrence of pregnancy failure [16, 17].

To confirm the bioinformatics predictions, both *DHFR* and *TYMS* 3'UTR containing *miR-196a-3p* binding sites were cloned into pmiR-GLO vector for luciferase assay. Transfection efficiency of *miR-196a-3p* mimic or inhibitor was detected by qRT-PCR shown in **Figure 3C**, *miR-*

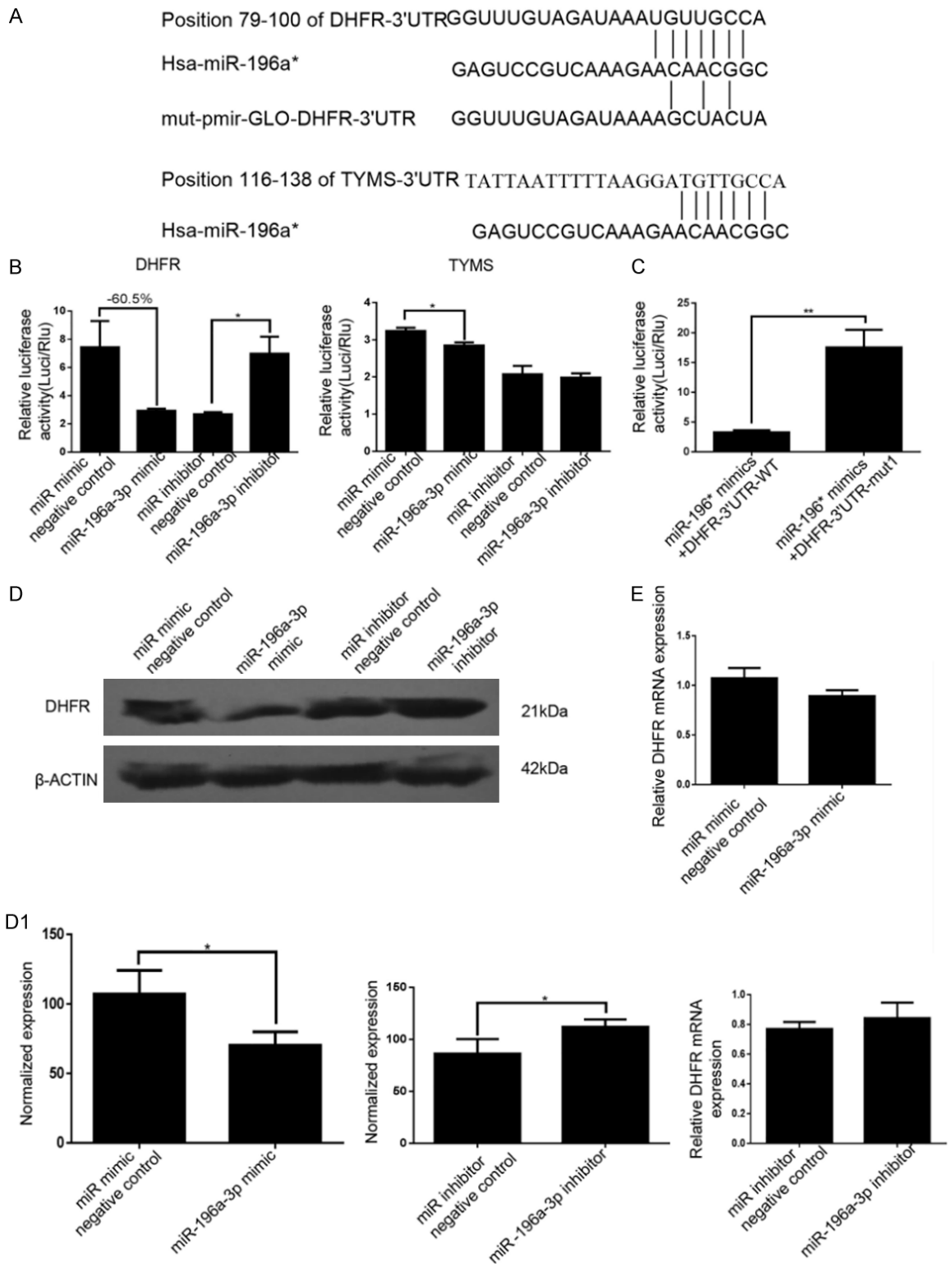

Figure 4. *MiR-196a-3p* directly targets the 3'-UTR of DHFR and represses its expression. (A) *miR-196a-3p* binding sites in the 3'-UTR region of *DHFR* and TYMS were predicted by TrargetScan. (B) HEK-293T cells were co-transfected with *miR-196a-3p* mimic or inhibitor and *DHFR*-pmiRGLO or TYMS-pmiRGLO for dual-luciferase assay. (C) HEK-293T cells were co-transfected with *miR-196a-3p* mimic and *DHFR*-pmiRGLO or *DHFR*-pmiRGLO-mut for dual-luciferase assay. DHFR protein and mRNA level was inhibited by miR-196a-3p mimic and promoted by *miR-196a-3p* inhibitor in western blotting (D and D1) and qRT-PCR (E). β-ACTIN was served as an internal control. **P*<0.05, ***P*<0.01.

196a-3p mimic could significantly increase and inhibitor could decrease its expression. As shown in **Figure 4B**, *miR-196a-3p* over-expression could significantly attenuated the luciferase activity of *DHFR*-pmiR-GLO by 60.5% in HTR-8/SVneo cells, while mutation of the seed sequence of *miR-196a-3p* blocked the inhibitory effect of *miR-196a-3p* on *DHFR* (**Figure 4C**). Conversely, *miR-196a-3p* antagonist could significantly increase the reporter activities of *DHFR*. In contrast, although *miR-196a-3p* mimic could significantly decrease the luciferase activity of *TYMS*-pmiR-GLO, but *miR-196a-3p* inhibitor could not reverse the inhibitory effect (**Figure 4B**). All these results indicate that *miR-196a-3p* targets the 3'UTR of *DHFR*.

To further identify the role of *miR-196a-3p* on the expression of *DHFR*, we next examined *DHFR* mRNA and protein after transfected HTR-8/SVneo cells with *miR-196a-3p* mimic or inhibitor. QRT-PCR results indicated that *miR-196a-3p* could slightly inhibit the level of *DHFR* mRNA, and *miR-196a-3p* inhibitor could slightly increase its mRNA expression (**Figure 4E**). Western blotting shown that *miR-196a-3p* could significantly inhibit the level of *DHFR* protein, while treatment with *miR-196a-3p* inhibitor resulted in increasing protein expression of *DHFR* (**Figure 4D**). Moreover, we found that the expression level of *DHFR* was inverted with that of *miR-196a-3p* in HEK-293, HEK-293T, Hela and HTR-8/SVneo cells (**Figure 1H**). *DHFR* is an important enzyme that reduces dihydrofolic acid to tetrahydrofolic acid, *miR-196a-3p* could influence folic acid metabolism by targeting *DHFR*.

MiR-196a-2 rs11614913 TT represses DHFR expression

To study whether *miR-196a-2* rs11614913 affect *DHFR* expression, *DHFR*-pmiRGLO or *DHFR*-pmiRGLO-mut was transfected into cells together with empty PCR3.1, *miR-196a-2*-T/T, *miR-196a-2*-C/C or *miR-196a-2*-T/C (**Figure 5A**). While transfected HTR-8/SVneo cells with *DHFR*-pmiRGLO-mut, the luciferase activity was significant higher than that with *DHFR*-pmiRGLO ($P<0.01$). When cells were co-transfected with different genotypes and *DHFR*-pmiRGLO, *miR-196a-2*-T/T significantly reduced the luciferase activity compared with *miR-196a-2*-C/C ($P<0.05$). All these facts reveal that *miR-196a-2* rs11614913 T/T represses *DHFR* expression.

MiR-196a-2 rs11614913 T/T attenuates the sensibility to progesterone antagonist mifepristone

In order to analyze the sensibility of different genotypes on the abortion and its therapeutic drug, cells transfected with different genotypes were treated by mifepristone or/and progesterone, and then cell proliferation was detected by MTT assay (**Figure 5D**). Different concentration mifepristone or progesterone was added to HTR-8/SVneo cells for MTT assays to identify the suitable concentration (**Figure 5B**, **5C**). Finally, 50 μM mifepristone and 0.1 μM progesterone were used in the following study. The results from MTT assay showed that 50 μM mifepristone treatment inhibited the cell proliferation induced by C/C homozygote ($P<0.05$), but had no significant effect on T/T homozygote. C/C homozygote-mediated the increase of cell viability was further reinforced by 0.1 μM progesterone treatment, and T/T homozygote-mediated the decrease of cell viability was rescued by 0.1 μM progesterone treatment. Additionally, progesterone treatment could partially restore the inhibition of cell proliferation-mediated by mifepristone in cells transfected with C/C homozygote and T/T homozygote. All these facts display that C allele is sensitive to mifepristone and progesterone, T allele is not responsive to mifepristone but is sensitive to progesterone.

Discussion

In the present study, we found that *miR-196a-2* rs11614913 T/T is associated with an increased risk of unexplained RPL. Subjects with rs11614913 T/T genotype had a higher RSA risk compared with subjects carrying C/C genotype. Rs11614913 showed a marginal association in dominant model (C/T+T/T vs. C/C) and significant association in a recessive model. Our results differ from previous study. Jeon reported that miR-196a2CC, miR-499AG+GG, and the miR-196a2CC/miR-499AG+GG combination was associated with increased risk of idiopathic RSA in Korean women [13], and chromosomally normal spontaneously aborted fetuses had significantly different frequencies of the miR-196a2CC, miR-146aCC/miR-196a2CC, and miR-149TT/miR-196a2CC genotypes compared with control subjects [18]. Parveen reported that miR-196a2CC, miR-499AG+GG and the miR-196a2CC/miR-499AG+GG along with some of the haplotypes combinations are asso-

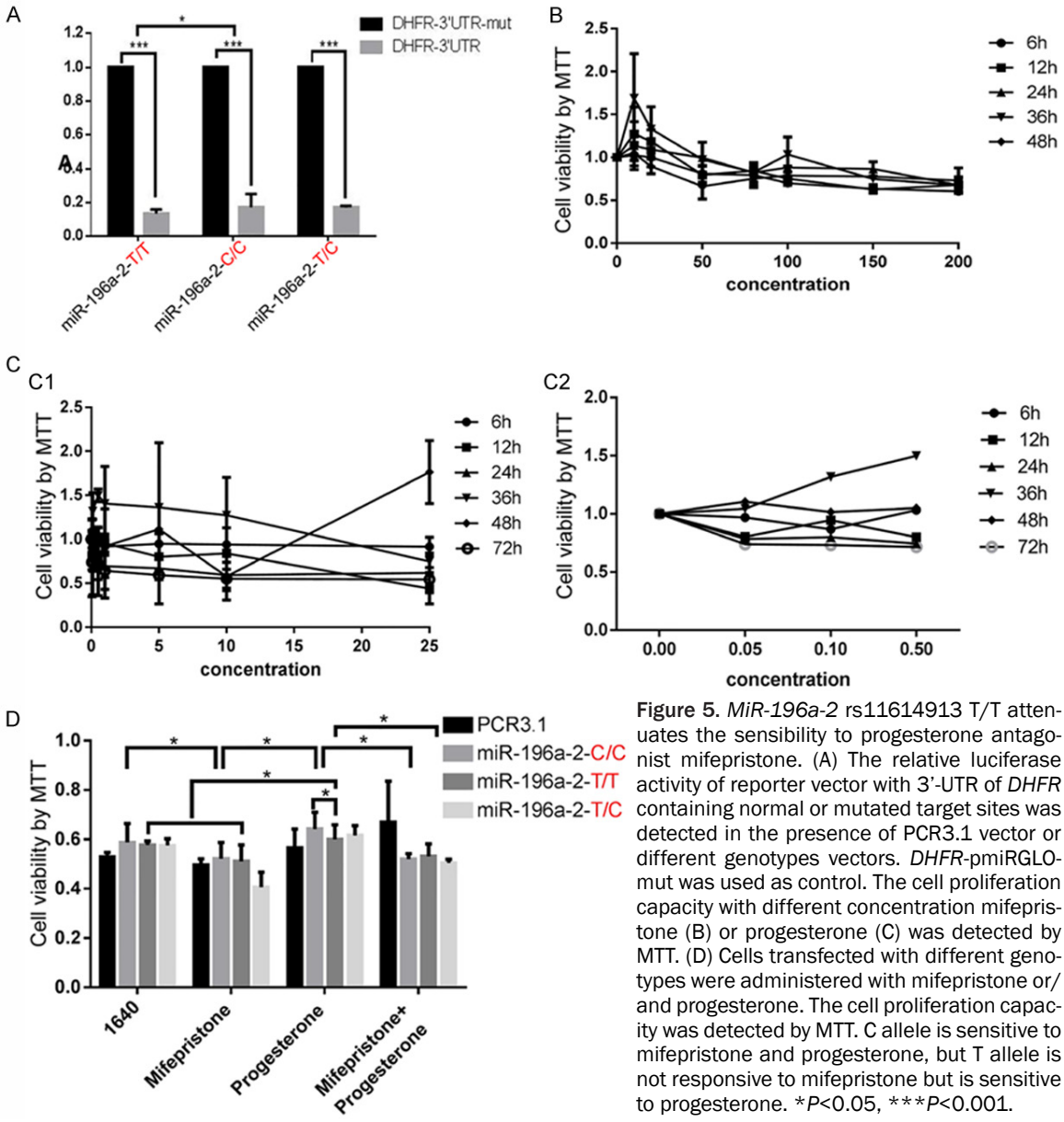

Figure 5. *MiR-196a-2* rs11614913 T/T attenuates the sensibility to progesterone antagonist mifepristone. (A) The relative luciferase activity of reporter vector with 3'-UTR of *DHFR* containing normal or mutated target sites was detected in the presence of PCR3.1 vector or different genotypes vectors. *DHFR*-pmiRGLO-mut was used as control. The cell proliferation capacity with different concentration mifepristone (B) or progesterone (C) was detected by MTT. (D) Cells transfected with different genotypes were administered with mifepristone or/and progesterone. The cell proliferation capacity was detected by MTT. C allele is sensitive to mifepristone and progesterone, but T allele is not responsive to mifepristone but is sensitive to progesterone. **P*<0.05, ****P*<0.001.

ciated with increased risk of recurrent miscarriage (RM) in North Indian Women [19]. Our results are consistent with reports from Amin-Beidokhti [20], their results indicated that the frequency of the miR-196a2 T allele was significantly higher in the women with RSA in comparison with the women in the control group. Ethnic effects may interpret the differences.

The secondary structure prediction showed that C to T substitution in *miR-196a-2* rs11614913 didn't alter the loop location but descended the predicted ΔG, suggesting the stability of construction was slightly destroyed. Chang reported that a C to U (T) change in pre-miR196a-2 generated an additional loop in the hairpin structure, leading to reduced stability and a smaller amount of the mature miR196a-2 [21]. Our results are inconsistent with this report, algorithm and the length of sequence may resulted in this difference. Therefore, we speculated that *miR-196a-2* rs11614913 might influenced the expression level of *miR-196a-5p* or *miR-196a-3p*. *MiR-196a-2* rs11614913 C>T significantly increased the expression of *miR-196a-3p* but not influenced the

expression of *miR-196a-5p*. Hoffman demonstrated that this variant led to less efficient processing of the miRNA precursor to its mature form, as well as diminished capacity to regulate target genes [22].

MiR-196a-2 rs11614913 has been associated with various types of cancer [23], suggesting that it may have effects on RSA via cell proliferation since the root cause of cancer is aberrant cell cycle regulation [24]. Association between the polymorphisms of the cell cycle-related genes TP53 and MDM2 and RSA supporting that cell proliferation plays an important role in RSA [25, 26]. Renthal demonstrated that certain miRNAs can modulate uterine quiescence and contractility during pregnancy and labor [22]. In this study, we found that *miR-196a-2* rs11614913 T/T significantly inhibited HTR-8/SVneo cells proliferation compared with C/C homozygote and T/C heterozygosity. The cell apoptotic level in early stage in *miR-196a-2*-T/T was obviously higher than that in *miR-196a-2*-C/C. Moreover, *miR-196a-2*-T/T in pre-*miR-196a-2* represses cell migration. While miR-196a-2-C/C represses cell invasion compared with miR-196a-2-T/T. Matrigel contains transforming growth factor β (TGF-β) and it is reported that TGF-β could down-regulate miR-196a-3p expression [27]. It is unknown that whether TGF-β from matrigel used in invasion assay may influence miR-196a-3p expression level or not, and then further affects miR-196a-2-C/C and miR-196a-2-T/T function on cell invasion. All these facts show that C allele positively regulate cell proliferation and migration, but T allele can attenuate the C allele-mediated reinforcement effects on cell growth and metastasis by reinforcing *miR-196a-3p* expression.

Ryan revealed that *miR-196a-2* is closely associated with cellular proliferation and differentiation [23]. It has been demonstrated that up-regulation of *miR-196a-2* affects mRNA expression of the HOX family of genes and Akt signaling [28, 29], which are linked to endometriosis [30] and miscarriages [13]. To further explore the possible molecular mechanisms of *miR-196a-2* rs11614913 T/T executing function, the binding status of *miR-196a-2* rs11614913 and its target gene was analyzed. *DHFR* was confirmed to be the target gene of *miR-196a-3p* by luciferase reporter assay and western blot. Luciferase reporter assay suggested that the T allele could more effectively suppress the expression of *DHFR* than C allele. Taken all these together, we speculate that T allele may not favorable to endometrial development by inhibiting cell growth, and then result in the increase of the risk of RSA acquisition.

In order to further research the possible reasons that C to T substitution in *miR-196a-2* rs11614913 increased the risk of RSA, we analyzed the sensibility of different genotypes on the abortion and its therapeutic drug. Mifepristone is a progesterone receptor antagonist used as an abortifacient in the first months of pregnancy, which can inhibit cell proliferation. Progesterone is beneficial to pregnancy and effective in the treatment of threatened miscarriage due to the decrease of progesterone. We found that C allele was more sensitive to mifepristone and progesterone than T allele, and C to T substitution attenuated the sensibility of cells to mifepristone. Therefore, we speculate that *miR-196a-2* rs11614913 T/T in pri-*miR-196a* may be able to inhibit the functions of progesterone, and then result in the increase of the risk of RSA acquisition.

In conclusion, this study first discovered that *miR-196a-2* rs11614913 T/T is associated with the increase the risk of RSA in northern Chinese Han population by down-regulating the expression of *miR-196a-3p* and up-regulating *DHFR*. Our discovery may give new insight into understanding of RSA development and mechanism, but also provide an opportunity to approach the problem of diagnosis and treatment of URSA.

Acknowledgements

This work was supported by grants from The National Key Research and Development Program of China (2016YFC1000307), the National Natural Science Foundation of China (No. 81771590) and CAMS Innovation Fund for Medical Sciences (CIFMS) (2018-I2M-1-004).

Disclosure of conflict of interest

None.

Address correspondence to: Xu Ma and Hongfei Xia, Reproductive and Genetic Center National Research Institute for Family Planning, 12 Dahuisi Road, Haidian, Beijing 100081, China. Tel: +86-010-621789-

32; Fax: +86-010-62179059; E-mail: genetic@263.net.cn (XM); hongfeixia@126.com (HFX)

References

[1] Practice Committee of American Society for Reproductive Medicine. Definitions of infertility and recurrent pregnancy loss: a committee opinion. Fertil Steril 2013; 99: 63.

[2] Lamont K, Scott NW, Jones GT and Bhattacharya S. Risk of recurrent stillbirth: systematic review and meta-analysis. BMJ 2015; 350: h3080.

[3] Dong F, Zhang Y, Xia F, Yang Y, Xiong S, Jin L and Zhang J. Genome-wide miRNA profiling of villus and decidua of recurrent spontaneous abortion patients. Reproduction 2014; 148: 33-41.

[4] Fejzo MS, Sazonova OV, Sathirapongsasuti JF, Hallgrimsdottir IB, Vacic V, MacGibbon KW, Schoenberg FP, Mancuso N, Slamon DJ and Mullin PM; 23andMe Research Team. Placenta and appetite genes GDF15 and IGFBP7 are associated with hyperemesis gravidarum. Nat Commun 2018; 9: 1178.

[5] Vaiman D. Genetic regulation of recurrent spontaneous abortion in humans. Biomed J 2015; 38: 11-24.

[6] Shomer E, Katzenell S, Zipori Y, Sammour RN, Isermann B, Brenner B and Aharon A. Microvesicles of women with gestational hypertension and preeclampsia affect human trophoblast fate and endothelial function. Hypertension 2013; 62: 893-898.

[7] Mendell JT and Olson EN. MicroRNAs in stress signaling and human disease. Cell 2012; 148: 1172-1187.

[8] Duan R, Pak C and Jin P. Single nucleotide polymorphism associated with mature miR-125a alters the processing of pri-miRNA. Hum Mol Genet 2007; 16: 1124-1131.

[9] Saunders MA, Liang H and Li WH. Human polymorphism at microRNAs and microRNA target sites. Proc Natl Acad Sci U S A 2007; 104: 3300-3305.

[10] Wang X, Li B, Wang J, Lei J, Liu C, Ma Y and Zhao H. Evidence that miR-133a causes recurrent spontaneous abortion by reducing HLA-G expression. Reprod Biomed Online 2012; 25: 415-424.

[11] Hu Z, Chen J, Tian T, Zhou X, Gu H, Xu L, Zeng Y, Miao R, Jin G, Ma H, Chen Y and Shen H. Genetic variants of miRNA sequences and non-small cell lung cancer survival. J Clin Invest 2008; 118: 2600-2608.

[12] Xiong XD, Cho M, Cai XP, Cheng J, Jing X, Cen JM, Liu X, Yang XL and Suh Y. A common variant in pre-miR-146 is associated with coronary artery disease risk and its mature miRNA expression. Mutat Res 2014; 761: 15-20.

[13] Jeon YJ, Choi YS, Rah H, Kim SY, Choi DH, Cha SH, Shin JE, Shim SH, Lee WS and Kim NK. Association study of microRNA polymorphisms with risk of idiopathic recurrent spontaneous abortion in Korean women. Gene 2012; 494: 168-173.

[14] Masterson JE and Schwartz SD. Evolution alters the enzymatic reaction coordinate of dihydrofolate reductase. J Phys Chem B 2015; 119: 989-996.

[15] Brunn ND, Dibrov SM, Kao MB, Ghassemian M and Hermann T. Analysis of mRNA recognition by human thymidylate synthase. Biosci Rep 2014; 34: e00168.

[16] Hobbs CA, Cleves MA, Macleod SL, Erickson SW, Tang X, Li J, Li M, Nick T and Malik S. Conotruncal heart defects and common variants in maternal and fetal genes in folate, homocysteine, and transsulfuration pathways. Birth Defects Res A Clin Mol Teratol 2014; 100: 116-126.

[17] Naithani M, Saxena V, Mirza AA, Kumari R, Sharma K and Bharadwaj J. Assessment of folic acid supplementation in pregnant women by estimation of serum levels of tetrahydrofolic acid, dihydrofolate reductase, and homocysteine. Scientifica (Cairo) 2016; 2016: 1520685.

[18] Jeon YJ, Kim SY, Rah H, Choi DH, Cha SH, Yoon TK, Lee WS, Shim SH and Kim NK. Association of the miR-146aC>G, miR-149T>C, miR-196a2T>C, and miR-499A>G polymorphisms with risk of spontaneously aborted fetuses. Am J Reprod Immunol 2012; 68: 408-417.

[19] Parveen F and Agrawal S. Recurrent miscarriage and micro-RNA among north Indian women. Reprod Sci 2015; 22: 410-415.

[20] Amin-Beidokhti M, Mirfakhraie R, Zare-Karizi S and Karamoddin F. The role of parental microRNA alleles in recurrent pregnancy loss: an association study. Reprod Biomed Online 2017; 34: 325-330.

[21] Chang CY, Lai MT, Chen Y, Yang CW, Chang HW, Lu CC, Chen CM, Chan C, Chung C, Tseng CC, Hwang T, Sheu JJ and Tsai FJ. Up-regulation of ribosome biogenesis by MIR196A2 genetic variation promotes endometriosis development and progression. Oncotarget 2016; 7: 76713-76725.

[22] Hoffman AE, Zheng T, Yi C, Leaderer D, Weidhaas J, Slack F, Zhang Y, Paranjape T and Zhu Y. microRNA miR-196a-2 and breast cancer: a genetic and epigenetic association study and functional analysis. Cancer Res 2009; 69: 5970-5977.

[23] Ryan BM, Robles AI and Harris CC. Genetic variation in microRNA networks: the implications for cancer research. Nat Rev Cancer 2010; 10: 389-402.

[24] Malumbres M and Carnero A. Cell cycle deregulation: a common motif in cancer. Prog Cell Cycle Res 2003; 5: 5-18.
[25] Fang Y, Kong B, Yang Q, Ma D and Qu X. MDM2 309 polymorphism is associated with missed abortion. Hum Reprod 2009; 24: 1346-1349.
[26] Pietrowski D, Bettendorf H, Riener EK, Keck C, Hefler LA, Huber JC and Tempfer C. Recurrent pregnancy failure is associated with a polymorphism in the p53 tumour suppressor gene. Hum Reprod 2005; 20: 848-851.
[27] Chen Y, Huang S, Wu B, Fang J, Zhu M, Sun L, Zhang L, Zhang Y, Sun M, Guo L and Wang S. Transforming growth factor-beta1 promotes breast cancer metastasis by downregulating miR-196a-3p expression. Oncotarget 2017; 8: 49110-49122.
[28] Makker A, Goel MM, Das V and Agarwal A. PI3K-Akt-mTOR and MAPK signaling pathways in polycystic ovarian syndrome, uterine leiomyomas and endometriosis: an update. Gynecol Endocrinol 2012; 28: 175-181.
[29] Vitiello D, Kodaman PH and Taylor HS. HOX genes in implantation. Semin Reprod Med 2007; 25: 431-436.
[30] Renthal NE, Chen CC, Williams KC, Gerard RD, Prange-Kiel J and Mendelson CR. miR-200 family and targets, ZEB1 and ZEB2, modulate uterine quiescence and contractility during pregnancy and labor. Proc Natl Acad Sci U S A 2010; 107: 20828-20833.